Dependence of the two-photon photoluminescence yield of gold nanostructures on the laser pulse duration

P. Biagioni,[1] M. Celebrano,[2,*] M. Savoini,[1] G. Grancini,[2] D. Brida,[2] S. Mátéfi-Tempfli,[3] M. Mátéfi-Tempfli,[3] L. Duò,[1] B. Hecht,[4] G. Cerullo,[2] and M. Finazzi[1,†]

[1]*Dipartimento di Fisica, LNESS, Politecnico di Milano, Piazza Leonardo da Vinci 32, 20133 Milano, Italy*

[2]*Dipartimento di Fisica, ULTRAS–INFM–CNR, Politecnico di Milano, Piazza Leonardo da Vinci 32, 20133 Milano, Italy*

[3]*Unité de Physico–Chimie et de Physique des Matériaux, Université Catholique de Louvain, Place Croix du Sud 1, 1348 Louvain-la-Neuve, Belgium*

[4]*Department of Experimental Physics 5, Nano-Optics & Biophotonics Group, Wilhelm-Conrad-Röntgen-Center for Complex Material Systems (RCCM), Physics Institute, University of Würzburg, Am Hubland, D-97074 Würzburg, Germany*

(Received 11 June 2009; published 14 July 2009)

Two-photon photoluminescence (TPPL) from gold nanostructures is becoming one of the most relevant tools for plasmon-assisted biological imaging and photothermal therapy as well as for the investigation of plasmonic devices. Here we study the yield of TPPL as a function of the temporal width δ of the excitation laser pulses for a fixed average power. In the $\delta > 1$ ps regime, the TPPL yield decreases as δ is increased, while for shorter pulse widths it becomes independent of δ and, consequently, of the laser-pulse peak power. This peculiar dynamics is understood and modeled by considering that two-photon absorption in Au is a two-step process governed by the lifetime of the metastable state populated by the first photon absorption.

DOI: 10.1103/PhysRevB.80.045411 PACS number(s): 78.67.Bf, 42.65.Sf, 73.22.Lp, 78.47.J−

I. INTRODUCTION

Since its introduction about 20 years ago,[1] two-photon microscopy has become a fundamental tool in high-resolution imaging, especially of biological tissues, because of the quadratic dependence of absorption on the excitation intensity, which confines fluorescence and photobleaching to the very proximity of the focal volume. Two-photon photoluminescence (TPPL) from molecules is a nonlinear process described by a third-order susceptibility tensor $\chi^{(3)}$ and the rate of absorption of energy is quadratically dependent on the laser intensity.[2] It is, therefore, usually investigated with ultrashort laser pulses, exploiting their very high peak powers. In particular, for a given average power, the TPPL yield usually scales as the peak intensity, or equivalently, as the inverse of the pulse temporal width δ.

Gold nanostructures often display strong multiphoton absorption,[3–9] which derives from the large electric fields that can be locally induced at their surface due to lightning-rod effects or collective electron oscillations.[10] Indeed, in recent years, the use of noble-metal nanoparticles has emerged as a valid and nontoxic alternative to fluorophore-based labeling for *in vitro* and *in vivo* imaging.[11] A most relevant application in this field is high-resolution analysis of tumor tissues with targeted gold nanoparticles,[12–14] which holds promise for superior contrast and increased biocompatibility. The appeal of such an approach lies also in the possibility to exploit the same nanoparticles for localized and enhanced photothermal therapies.[15,16] The strong nonlinear optical response can also be employed as an effective tool to map spatially localized field-amplitude enhancements in nanostructured systems. In particular, TPPL microscopy is now recognized as one of the most efficient ways to probe and image plasmon modes in single gold nanoparticles[8,17–19] and resonant optical antennas.[4,20,21]

Despite the great number of scientific works addressing and exploiting nonlinear absorption in Au nanostructures, scarce information exists about its pulse-duration dependence. A pulse-width-dependent nonlinearity in optical absorption has been investigated in Au films[22] and in embedded Au nanoparticles.[23] In the first case, the nonlinearity directly arises from thermal smearing of the electronic distribution due to large excitation fluencies. In the second case, a saturation of the nonlinear-absorption coefficient with pulse shortening is attributed to reduced contributions from slow processes in the nonlinear response of the system.

In this work we show that the TPPL yield excited in Au nanostructures by ultrashort light pulses does not scale with the expected $1/\delta$ pulse width dependence. In particular, for pulse widths shorter than about 1 ps, the TPPL counting rate obtained for a given pulse energy does not show any sizeable dependence on the pulse peak power. This unexpected finding holds important consequences for gold-based nanophotonics and can be understood by considering that two-photon absorption in gold is a two-step process consisting of two successive one-photon steps, as recently proposed by Imura *et al.*,[8] with the lifetime of the intermediate state, after the first photon absorption, ruling TPPL dynamics. The analysis by Imura *et al.* was supported by the TPPL polarization dependence, which was, however, questioned by later experimental results,[12,13,24] so that a strong support to their interpretation is still missing.

II. SAMPLE AND EXPERIMENTAL SETUP

Our sample consists of an array of gold nanowires obtained by electrochemical growth in a supported nanoporous aluminum oxide template.[25] The wires have typically 50–70 nm width, 300–600 nm length, and about 100 nm interaxis separation (see Fig. 1). In agreement with similar samples described in the literature,[26] the wires display a broad longitudinal surface-plasmon-polariton (SPP) resonance in the near infrared, which partially overlaps with the

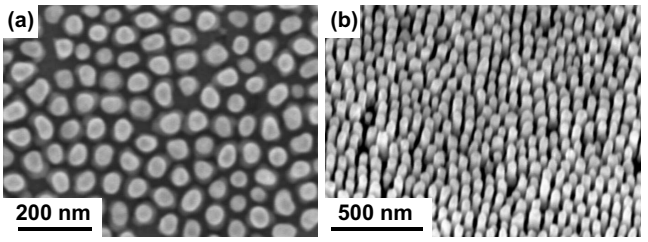

FIG. 1. Representative SEM images of the sample used for the experiments: top view (a) and side view (b).

wavelength of the laser source used to excite TPPL.

The pulsed light source used for TPPL measurements consists of a long-cavity mode-locked Ti:sapphire oscillator (26 MHz repetition rate) producing 40 fs pulses at $\lambda_{ex}=800$ nm. The pulse duration δ is varied by introducing a negative chirp with dispersive delay lines based on a double pass in either a pair of SF10 Brewster-cut prisms (to cover the $\delta<2$ ps range) or a pair of 600 lines/mm gratings ($\delta>1$ ps). TPPL is excited and collected by feeding the collimated laser beam into a 0.5 NA aspherical lens focused on the sample surface. The average power P_0 has been varied with a graduated neutral-density filter. The TPPL signal is separated from the background at the fundamental wavelength by a combination of shortpass filters (Schott BG39). A further longpass filter (cutoff around 415 nm) is inserted along the collection path to suppress possible second-harmonic generation from the sample.

Pump-probe spectroscopy provides experimental access to the value of relevant parameters used in the model to interpret our findings (see below). The pump-probe setup (see Fig. 2) is driven by a regeneratively amplified Ti:sapphire laser that delivers 150 fs pulses centered at 800 nm at 1 kHz repetition rate. We use the fundamental-frequency (FF) pulses to excite the gold sample while the white-light probe was generated by tightly focusing a small fraction of the FF pulse in a 2-mm-thick sapphire plate. Pump and probe pulses are synchronized with a motorized delay line and overlapped on the sample in a quasicollinear geometry. After the sample, each single pump-perturbed and unperturbed probe pulse is collected by a fast optical multichannel analyzer enabling us to retrieve a spectral map of the dynamics of the sample differential reflectivity $(\Delta R/R)$.[27]

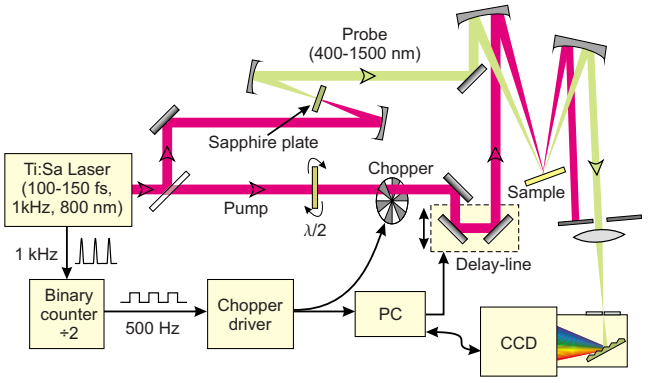

FIG. 2. (Color online) Sketch of the experimental setup for pump-probe spectroscopy.

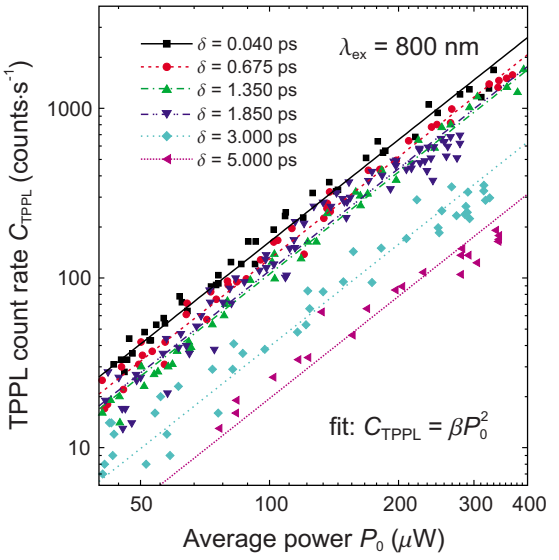

FIG. 3. (Color online) Selection of TPPL data as a function of the average power P_0 impinging on the sample and pulse duration δ. The excitation wavelength is $\lambda_{ex}=800$ nm. All data have been fitted with a quadratic law: $C_{TPPL}=\beta P_0^2$.

III. EXPERIMENTAL RESULTS AND DISCUSSION

Figure 3 reports the collected TPPL count rate C_{TPPL} as a function of the average power P_0 and pulse duration δ of the fundamental wavelength excitation. Each reported experimental curve is the result of averaging several spots on the sample. In the power range reported in Fig. 3, the sample does not show any sign of degradation and the collected intensity is very well reproducible as the incident power is varied over many cycles. From Fig. 3, one can immediately recognize a quadratic dependence of C_{TPPL} on P_0. Higher-order nonlinear effects, which have also been reported in gold nanostructures,[4–6] have not been observed over the investigated fluence range.

For each value of the pulse duration δ we evaluate the coefficient β defined by the relation $C_{TPPL}=\beta P_0^2$ that best fits the experimental data. The value of β is plotted in Fig. 4 as a function of δ. For pulse widths $\delta<1$ ps, β does not display any significant dependence on δ, meaning that, for a fixed incident average power, the TPPL yield becomes independent of the pulse peak power, in striking contrast with standard TPPL from, e.g., molecules. Similar results (not shown) have been obtained by also introducing a positive chirp by bulk propagation in optical fibers with different lengths.

In order to explain the trend of the β coefficient displayed in Fig. 4 we recall that, in gold nanostructures, TPPL has been proposed to generate from the recombination of an electron in the *sp* band with a hole in the 3*d* band, created by a two-step process consisting in two sequential one-photon absorption transitions.[8] As sketched in Fig. 5, the first photon excites an electron to the *sp* conduction band above the Fermi energy (E_F) via an intraband transition, leaving a hole in the *sp* conduction band located below E_F. Note that intraband transitions, which are dipole- forbidden in bulk materials, are characterized by large cross sections in nanostruc-

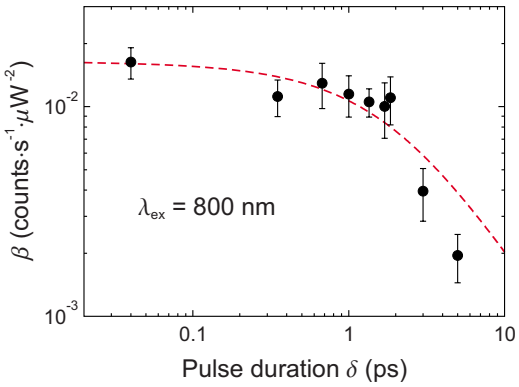

FIG. 4. (Color online) Pulse-duration dependence of the coefficient β evaluated by the quadratic fitting of C_{TPPL} as a function of P_0, as illustrated in Fig. 3. The error bars correspond to twice the standard deviation of C_{TPPL} with respect to the fitting. The dashed line corresponds to the result of the model discussed in the text.

tures because of the presence of intense evanescent fields, whose associated field gradients give rise to higher-order multipolar transitions.[3]

Once the *sp* hole has been created by the first photon, the second photon excites an electron from the *d* band to recombine with the *sp* hole in the conduction band. In gold crystals, this optical transition preferentially occurs near the *X* and *L* symmetry points of the Brillouin zone, since there the 3*d*-projected electronic density of states is larger. Before they recombine, both the *sp* and *d* holes may undergo scattering events. The excited *d* hole resulting from the two sequential one-photon absorption steps can, eventually, decay radiatively, directly contributing to generate TPPL, but can also recombine nonradiatively with *sp* electrons by generating SPPs that subsequently radiate, further contributing to the total luminescence yield.[28]

Because of the short hole-scattering times in the *d* and *sp* bands (about 100 fs, see Ref. 29), interband coherence can be ignored and the two successive one-photon absorption steps

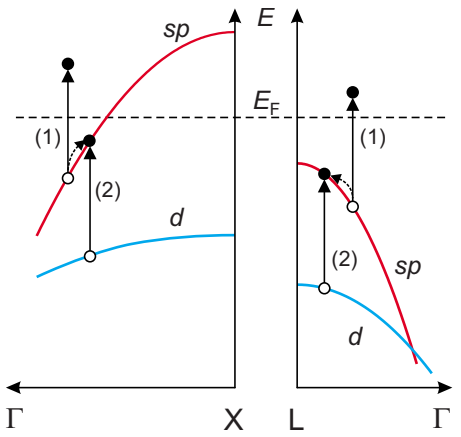

FIG. 5. (Color online) Two-photon-induced excitation of a 3*d* hole in gold, after Ref. 8. The first photon (1) induces an indirect $sp \rightarrow sp$ intraband transition. Then, absorption of the second photon (2) creates a hole in the *d* band by exciting an electron to recombine with the previously created *sp* hole.

sketched in Fig. 5 can be described by the following rate equations:

$$\frac{dN_{sp}}{dt} = \sigma_{sp\rightarrow sp} N F(t) - \frac{N_{sp}}{\tau_{sp}} - \sigma_{d\rightarrow sp} N_{sp} F(t), \tag{1a}$$

$$\frac{dN_d}{dt} = \sigma_{d\rightarrow sp} N_{sp} F(t) - \frac{N_d}{\tau_d}, \tag{1b}$$

where N is the electron density in the *sp* conduction band, N_{sp} and N_d are the densities of holes created below E_{F} in the *sp* and *d* bands, respectively, while τ_{sp} and τ_d represent the relaxation times of the *sp* and *d* holes. $F(t)$ is the instantaneous photon flux and $\sigma_{sp\rightarrow sp}(\sigma_{d\rightarrow sp})$ stands for the cross section of the first (second) absorption event illustrated in Fig. 5. The third term in the right-hand part of Eq. (1a), accounting for *sp*-hole recombination due to the $d \rightarrow sp$ absorption step, can be neglected in the small perturbation regime characterized by $N_{sp} \ll N$. Note that, due to the broad *sp* and *d* bandwidths, our model is independent of the sign of the pulse chirp, in agreement with observations.

Let us consider pulses of total energy E_{pulse}, repetition rate equal to ν_{rep}, and instant power equal to $E_{\mathrm{pulse}} h_\delta(t)$, being $h_\delta(t)$ a function normalized to unity that describes the temporal profile of each pulse. By solving Eq. (1) and taking the time average, in the limit $\tau_d \ll \nu_{\mathrm{rep}}^{-1}$, one obtains the following expression for the average hole density in the *d* band:

$$\langle N_d \rangle = (1-R)^2 E_{\mathrm{pulse}}^2 \nu_{\mathrm{rep}} \tau_d \left(\frac{\lambda_{\mathrm{ex}}^2}{h^2 c^2} \right) \left(\frac{\sigma_{sp\rightarrow sp} \sigma_{d\rightarrow sp}}{A^2} \right) N \times \int_{-\infty}^{\infty} h_\delta(t) dt \int_0^{\infty} e^{-t'/\tau_{sp}} h_\delta(t-t') dt'. \tag{2}$$

In this expression, A is the area of the laser spot on the sample and R is the sample reflectivity. Equation (2) describes the dependence of the time-averaged TPPL count rate on incident power and pulse duration, as the number of detected photons is proportional to the total number of *d* holes generated in the two-step process,[28] giving $C_{\mathrm{TPPL}} \propto \langle N_d \rangle$. As a consequence of Eq. (2), the TPPL intensity is expected to follow a quadratic dependence upon the average power P_0 impinging on the sample, $P_0 = \nu_{\mathrm{rep}} E_{\mathrm{pulse}}$, in agreement with the experimental data displayed in Fig. 3.

We are now in the position to discuss the dependence of C_{TPPL} upon δ. When $\delta \ll \tau_{sp}$, the exponential term in the double integral in Eq. (2) can be omitted, since it would not show any significant variation during the time interval corresponding to a nonvanishing pulse amplitude. Physically, this means that the probability that the created *sp* hole recombines within the same laser pulse is negligible. In this case one obtains that the TPPL intensity is proportional to the time integral of the pulse autocorrelation and does not depend on δ. Conversely, for $\delta \gg \tau_{sp}$, the two sequential one-photon absorption transitions can be practically considered as simultaneous events on the time scale defined by the pulse temporal width. The result in this case is that C_{TPPL} becomes proportional to the time integral of the squared energy of the pulse. One thus retrieves the expected limit characterized by a TPPL yield scaling as δ^{-1}.

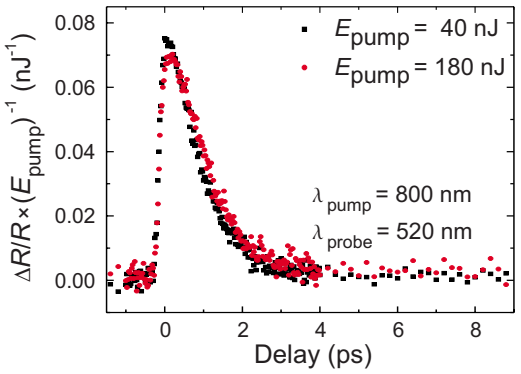

FIG. 6. (Color online) Plot of the differential reflectivity versus time acquired with a pump-probe setup using 800 nm wavelength pump and 520 nm wavelength probe.

The evolution of C_{TPPL} as a function of δ depends only very weakly on the details of the function $h_\delta(t)$ describing the temporal shape of the pulse. The dashed line that fits the experimental data in Fig. 4 has been obtained by assuming $h_\delta(t)=(\alpha/\delta)\mathrm{sech}^2(2\alpha t/\delta)$ ($\alpha=0.88$ to have δ corresponding to the pulse full width at half maximum), which corresponds to the mode-locking eigenfunction of the propagating pulse inside the laser cavity.

In order to experimentally obtain the value of τ_{sp}, we have measured the *sp*-hole lifetime by means of a standard pump-probe technique, with excitation wavelength at 800 nm and probe wavelength at 520 nm, a combination that probes the carrier lifetime in the conduction band.[29] A plot of $\Delta R/R$ versus time is shown in Fig. 6, with two different pump intensities providing the same response, as a proof that the electron temperature is not significantly changed and the system is in a small perturbation regime. The $\Delta R/R$ signal displays an exponential decay with time constant $\tau_{sp}\simeq 1$ ps, due to electron-electron and electron-phonon scattering, and a tail due to the much slower phonon-phonon thermalization. This is in good agreement with typical internal relaxation times observed for electrons and holes close to the Fermi level in gold films.[29,30] As illustrated by the fitting in Fig. 4, the result obtained from Eq. (2), with the measured value for τ_{sp} and only a scaling factor as a fitting parameter, correctly reproduces the trend of TPPL yield as a function of pulse width.

We have also evaluated the possible influence of thermal effects on the C_{TPPL} dependence upon P_0 and δ. The electron dynamics as a function of the laser fluence have been simulated by the two-temperature model for electrons and lattice.[29,31] We have considered two temperature-dependent effects, namely, (i) smearing of the Fermi distribution function[22] and (ii) thermally induced damping of the SPP resonance.[32,33] In the first case we obtain saturation effects associated with the high occupancy of the final states reached after the two sequential one-photon absorption steps. In the second case, the optical response of the nanostructures is smeared by thermally increased electron-electron scattering, which leads to damped SPP excitations and reduced local electric fields. In both cases thermal effects manifest themselves with a C_{TPPL} vs P_0 dependence that deviates from the quadratic law for high laser fluencies. We are thus confident that such effects are not relevant in the set of data presented in Fig. 3, albeit they can play a role when a higher excitation power is used.

IV. CONCLUSIONS

In conclusion, we have demonstrated that, for a given pulse energy, the TPPL yield in gold nanowires becomes independent of the pulse duration δ for laser pulses shorter than about 1 ps. For longer pulses, the TPPL intensity displays the expected asymptotical proportionality to $1/\delta$. This behavior is determined by the fact that TPPL in gold nanostructures is obtained after a $3d$ hole is produced by two sequential absorption steps involving a single photon and is governed by the lifetime of the *sp* conduction-band hole generated after the first photon absorption.

It is worth noticing that in TPPL microscopy great care is often taken to precompensate for positive dispersion introduced by the optical elements in the microscope, in order to achieve transform-limited pulses at the focal position. While this is always needed to ensure the best fluorescence intensity from dye molecules for a given average power, our work implies that precompensation techniques are not necessary for TPPL microscopy with gold nanoparticles. Moreover, ps pulses effectively avoid optical saturation and SPP bleaching, which can be a consequence of thermally increased electron-electron scattering.[22,32]

The peculiar dynamics highlighted in our work directly stems from the bulk band structure of Au and does not depend on the detailed shape and plasmon resonances of the nanostructure under investigation, therefore holding consequences for many applications in nano-optics, plasmonics, and bioimaging. Moreover, it provides a strong support to the two-step absorption mechanism proposed in previous publications.[8]

ACKNOWLEDGMENTS

The authors acknowledge D. Polli for assistance during the experimental sessions. This work was partially supported by the Interuniversity Attraction Pole Program (P6/42)-Belgian State-Belgian Science Policy.

*Present address: Laboratory of Physical Chemistry, ETH Zurich, HCI F 202, 8093 Zurich, Switzerland.
†marco.finazzi@fisi.polimi.it

[1] W. Denk, J. H. Strickler, and W. W. Webb, Science **248**, 73 (1990).
[2] J. D. Bhawalkar, G. S. He, and P. N. Prasad, Rep. Prog. Phys. **59**, 1041 (1996).
[3] M. R. Beversluis, A. Bouhelier, and L. Novotny, Phys. Rev. B

68, 115433 (2003).
[4] P. Mühlschlegel, H.-J. Eisler, O. J. F. Martin, B. Hecht, and D. W. Pohl, Science **308**, 1607 (2005).
[5] R. A. Farrer, F. L. Butterfield, V. W. Chen, and J. T. Fourkas, Nano Lett. **5**, 1139 (2005).
[6] Q.-Q. Wang, J.-B. Han, D.-L. Guo, S. Xiao, Y.-B. Han, H.-M. Gong, and X.-W. Zou, Nano Lett. **7**, 723 (2007).
[7] W. Dickson, P. R. Evans, G. A. Wurtz, W. Hendren, R. Atkinson, R. J. Pollard, and A. V. Zayats, J. Microsc. **229**, 415 (2008).
[8] K. Imura, T. Nagahara, and H. Okamoto, J. Phys. Chem. B **109**, 13214 (2005).
[9] C. Ropers, D. R. Solli, C. P. Schulz, C. Lienau, and T. Elsaesser, Phys. Rev. Lett. **98**, 043907 (2007).
[10] L. Novotny and B. Hecht, *Principles of Nano-Optics* (Cambridge University Press, Cambridge, 2006).
[11] D. Nagesha, G. S. Laevsky, P. Lampton, R. Banyal, C. Warner, C. DiMarzio, and S. Sridhar, Int. J. Nanomedicine **2**, 813 (2007).
[12] N. J. Durr, T. Larson, D. K. Smith, B. A. Korgel, K. Sokolov, and A. Ben-Yakar, Nano Lett. **7**, 941 (2007).
[13] H. Wang, T. B. Huff, D. A. Zweifel, W. He, P. S. Low, A. Wei, and J.-X. Cheng, Proc. Natl. Acad. Sci. U.S.A. **102**, 15752 (2005).
[14] L. Bickford, J. Sun, K. Fu, N. Lewinski, V. Nammalvar, J. Chang, and R. Drezek, Nanotechnology **19**, 315102 (2008).
[15] D. P. O'Neal, L. R. Hirsch, N. J. Halas, J. D. Payne, and J. L. West, Cancer Lett. **209**, 171 (2004).
[16] I. H. El-Sayed, X. Huang, and M. A. El-Sayed, Cancer Lett. **239**, 129 (2006).
[17] A. Bouhelier, M. R. Beversluis, and L. Novotny, Appl. Phys. Lett. **83**, 5041 (2003).
[18] A. Hohenau, J. R. Krenn, J. Beermann, S. I. Bozhevolnyi, S. G. Rodrigo, L. Martin-Moreno, and F. Garcia-Vidal, Phys. Rev. B **73**, 155404 (2006).
[19] K. Imura, T. Nagahara, and H. Okamoto, Appl. Phys. Lett. **88**, 023104 (2006).
[20] P. J. Schuck, D. P. Fromm, A. Sundaramurthy, G. S. Kino, and W. E. Moerner, Phys. Rev. Lett. **94**, 017402 (2005).
[21] P. Ghenuche, S. Cherukulappurath, T. H. Taminiau, N. F. van Hulst, and R. Quidant, Phys. Rev. Lett. **101**, 116805 (2008).
[22] N. Rotenberg, A. D. Bristow, M. Pfeiffer, M. Betz, and H. M. van Driel, Phys. Rev. B **75**, 155426 (2007).
[23] O. Plaksin, Y. Takeda, H. Amekura, N. Kishimoto, and S. Plaksin, J. Appl. Phys. **103**, 114302 (2008).
[24] H. Kim, C. Xiang, A. G. Güell, R. M. Penner, and E. O. Potma, J. Phys. Chem. C **112**, 12721 (2008).
[25] A. Vlad, M. Mátéfi-Tempfli, S. Faniel, V. Bayot, S. Melinte, L. Piraux, and S. Mátéfi-Tempfli, Nanotechnology **17**, 4873 (2006).
[26] G. A. Wurtz, W. Dickson, D. O'Connor, R. Atkinson, W. Hendren, P. Evans, R. Pollard, and A. V. Zayats, Opt. Express **16**, 7460 (2008).
[27] D. Polli, L. Lüer, and G. Cerullo, Rev. Sci. Instrum. **78**, 103108 (2007).
[28] E. Dulkeith, T. Niedereichholz, T. A. Klar, J. Feldmann, G. von Plessen, D. I. Gittins, K. S. Mayya, and F. Caruso, Phys. Rev. B **70**, 205424 (2004).
[29] C.-K. Sun, F. Vallée, L. H. Acioli, E. P. Ippen, and J. G. Fujimoto, Phys. Rev. B **50**, 15337 (1994).
[30] R. H. M. Groeneveld, R. Sprik, and A. Lagendijk, Phys. Rev. B **51**, 11433 (1995).
[31] S. I. Anisimov, B. L. Kapeliovich, and T. L. Perel'man, Zh. Eksp. Teor. Fiz. **66**, 776 (1974) [Sov. Phys. JETP **39**, 375 (1974)].
[32] M. Perner, P. Bost, U. Lemmer, G. von Plessen, J. Feldmann, U. Becker, M. Mennig, M. Schmitt, and H. Schmidt, Phys. Rev. Lett. **78**, 2192 (1997).
[33] M. Pelton, M. Liu, S. Park, N. F. Scherer, and P. Guyot-Sionnest, Phys. Rev. B **73**, 155419 (2006).